J. Fluid Mech. (2007), *vol.* 591, *pp.* 413–436.
doi:10.1017/S002211200700835X Printed in the United Kingdom

The near-shore behaviour of shallow-water waves with localized initial conditions

DAVID PRITCHARD[1] AND LAURA DICKINSON[2]

[1] Department of Mathematics, University of Strathclyde, 26 Richmond St, Glasgow G1 1XH, UK
dtp@maths.strath.ac.uk

[2] Division of Civil Engineering, University of Dundee, Dundee DD1 4HN, UK
l.dickinson@dundee.ac.uk

(Received 24 July 2006 and in revised form 20 July 2007)

We consider the behaviour of solutions to the nonlinear shallow-water equations which describe wave runup on a plane beach, concentrating on the behaviour at and just behind the moving shoreline. We develop regular series expansions for the hydrodynamic variables behind the shoreline, which are valid for any smooth initial condition for the waveform. We then develop asymptotic descriptions of the shoreline motion under localized initial conditions, in particular a localized Gaussian waveform: we obtain estimates for the maximum runup and drawdown of the wave, for its maximum velocities and the forces it is able to exert on objects in its path, and for the conditions under which such a wave breaks down. We show how these results may be extended to include initial velocity conditions and initial waveforms which may be approximated as the sum of several Gaussians. Finally, we relate these results tentatively to the observed behaviour of a tsunami.

1. Introduction

An important problem in coastal engineering and natural hazard mitigation is to describe the runup of long waves, such as tsunamis, on a sloping beach. Over the last fifty years several analytical and computational tools have been developed to model the runup process. The most common models employ the depth-averaged nonlinear shallow-water equations (NSWEs), which are valid as long as the length scale of the free surface motion is much greater than the fluid depth (Peregrine 1972). The NSWEs are frequently used in numerical models to predict the inundation of specific coastlines or to investigate wave-generation processes (e.g. Titov & Synolakis 1998; Tinti & Tonini 2005), as well as in more idealized situations to investigate the general principles of runup.

Carrier & Greenspan (1958) developed a useful analytical approach to the problem of runup on a plane beach, where the undisturbed fluid depth increases linearly with distance offshore. In this approach, a hodograph transformation is used to convert the NSWEs into a single linear equation in terms of 'distorted time' and 'distorted space' coordinates, and solutions can then be obtained by superposing modes. Particular solutions derived using this approach have been presented by several authors, including Synolakis (1987) and Tadepalli & Synolakis (1994); Carrier, Wu & Yeh (2003) were the first to present a general solution to the initial-value problem. Recently, Kânoğlu (2004) has demonstrated how to determine efficiently the shoreline motion of Carrier *et al.*'s solutions, and so to relate initial conditions directly to runup

distances, while Antuono & Brocchini (2007) have provided the first general solution to the boundary-value problem.

The shoreline solutions presented by Kânoğlu (2004) are in general form and so require a little effort to evaluate. The purpose of the present study is to develop asymptotically reduced descriptions of the shoreline and near-shore hydrodynamics for some commonly considered waveforms, and to use these to derive estimates for quantities of physical interest such as the shoreline excursion, the forces exerted by the wave on immersed bodies, and the conditions for the shallow-water description of the flow to remain valid. This follows the successful development by Synolakis (1987) and Tadepalli & Synolakis (1994) of asymptotic solutions to various boundary-value problems in a similar limit.

In § 2 we describe the nonlinear shallow-water model for flow over a plane beach, together with the hodograph transformation and the solutions derived by Carrier *et al.* (2003); we discuss breakdown (§ 2.2) and develop expressions for the hydrodynamic variables at the shoreline (§ 2.3). In § 3 we develop asymptotic results when the initial condition is a single Gaussian waveform; we compare the asymptotics with the shoreline variables under the full solution, and discuss the implications of our results. In § 4 we extend these ideas to 'N-waves' composed of two Gaussians with different sign, paying particular attention to the maximum runup and drawdown of the shoreline and to the conditions for breakdown of these solutions. Finally, in § 5 we examine our predictions in the light of field data for a tsunami, and discuss their contribution to the general area of wave runup modelling.

2. Mathematical development

2.1. *Description of the model and the hodograph transformation*

The NSWEs for flow over a beach inclined at a uniform angle α from the horizontal are given by

$$\frac{\partial \hat{\eta}}{\partial \hat{t}} + \frac{\partial}{\partial \hat{x}}\left[\bar{u}\left(\hat{x}\tan\alpha + \hat{\eta}\right)\right] = 0, \quad \frac{\partial \bar{u}}{\partial \hat{t}} + \bar{u}\frac{\partial \bar{u}}{\partial \hat{x}} + \hat{g}\frac{\partial \hat{\eta}}{\partial \hat{x}} = 0, \tag{2.1}$$

where $\hat{\eta}$ is the surface elevation above mean sea level, $\bar{u}$ is the depth-averaged horizontal velocity, $\hat{g}$ is the acceleration due to gravity and $\hat{x}$ is a horizontal coordinate increasing offshore and with origin at the undisturbed shoreline. We may choose some characteristic horizontal length scale $\hat{L}$ and define non-dimensional variables by

$$\hat{x} = \hat{L}x, \quad \hat{t} = \sqrt{\frac{\hat{L}}{\hat{g}\tan\alpha}}t, \quad \hat{\eta} = (\hat{L}\tan\alpha)\eta, \quad \bar{u} = \sqrt{\hat{g}\hat{L}\tan\alpha}u, \tag{2.2}$$

to obtain the dimensionless NSWEs (also known as the 'beach equations')

$$\frac{\partial \eta}{\partial t} + \frac{\partial}{\partial x}\left[u\left(x+\eta\right)\right] = 0, \quad \frac{\partial u}{\partial t} + u\frac{\partial u}{\partial x} + \frac{\partial \eta}{\partial x} = 0. \tag{2.3}$$

The length scale $\hat{L}$ may be left indeterminate (see the discussion by Meyer 1986*a*, *b*). For our purposes, it is convenient to define it in terms of the initial conditions of the waveforms we will investigate: we will assume that $\hat{L}$ has been chosen to coincide with some measure of the initial position of the waveform, and remark on it on a case-by-case basis. It should also be noted at this point that because we consider only a plane beach, if our results are to be related to more complex bathymetries (such as that considered by Synolakis 1987) we must restrict our analysis to cases where the

initial waveform is within the region of constant gradient, so the 'toe' of the beach lies seaward of $\hat{x} = \hat{L}$.

To carry out the hodograph transform, we define the new independent variables $\lambda = t - u$ and $q = x + \eta$; we subsequently define $\sigma = \sqrt{q}$, noting that $q > 0$ throughout the fluid domain, and that $\sigma = 0$ represents the moving shoreline. (We will denote quantities evaluated at $\sigma = 0$ by a subscript '*sh*'.) We may now define a potential $\phi(\sigma, \lambda)$ such that

$$\eta + \frac{1}{2}u^2 = \frac{\partial \phi}{\partial \lambda}, \quad \text{and hence} \quad u = -\frac{1}{2\sigma}\frac{\partial \phi}{\partial \sigma} \quad \text{and} \quad \eta = \frac{\partial \phi}{\partial \lambda} - \frac{1}{8\sigma^2}\left(\frac{\partial \phi}{\partial \sigma}\right)^2, \tag{2.4}$$

and combine the transformed NSWEs to obtain the single linear governing equation

$$4\sigma \frac{\partial^2 \phi}{\partial \lambda^2} - \frac{\partial}{\partial \sigma}\left(\sigma \frac{\partial \phi}{\partial \sigma}\right) = 0. \tag{2.5}$$

The Jacobian of the transformation from (x, t) to (q, λ) may be written in terms of σ and λ as

$$J = -\frac{1}{8\sigma^4}\left(\frac{\partial \phi}{\partial \sigma}\right)^2 + \frac{1}{8\sigma^3}\left(\frac{\partial^2 \phi}{\partial \sigma^2} + 2\frac{\partial^2 \phi}{\partial \lambda^2}\right)\frac{\partial \phi}{\partial \sigma} - \frac{1}{4\sigma^2}\left[\frac{\partial^2 \phi}{\partial \sigma^2}\frac{\partial^2 \phi}{\partial \lambda^2} - \left(\frac{\partial^2 \phi}{\partial \lambda \partial \sigma}\right)^2\right] - \frac{1}{\sigma}\frac{\partial^2 \phi}{\partial \lambda \partial \sigma} + 1. \tag{2.6}$$

This quantity is often referred to simply as 'the Jacobian' of the hodograph transformation (e.g. Synolakis 1987; Carrier *et al.* 2003); in contrast, Carrier & Greenspan (1958) deal with the true Jacobian of the transformation $(x, t) \mapsto (\sigma, \lambda)$, which is given in our notation by $2\sigma J$. We will follow the terminology of the more recent studies, but bearing this caveat in mind.

Carrier *et al.* (2003) developed solutions to (2.5) using a Fourier–Bessel transform, so the individual modes are sinusoidal in the 'time' variable λ, and take the form of Bessel functions in the 'space' variable σ. Taking the general initial condition

$$\phi(\sigma, 0) = P(\sigma) = -\int_0^\sigma 2\sigma' u(\sigma', 0)\, \mathrm{d}\sigma', \quad \frac{\partial \phi}{\partial \lambda}(\sigma, 0) = F(\sigma) = \eta(\sigma, 0) + \frac{1}{2}u^2(\sigma, 0), \tag{2.7}$$

we may obtain (cf. equation (19) of Carrier *et al.* 2003)

$$\phi(\sigma, \lambda) = \int_0^\infty \int_0^\infty \zeta J_0(\rho\sigma) J_0(\rho\zeta)\left[2\sin\left(\frac{\lambda}{2}\rho\right)F(\zeta) + \rho\cos\left(\frac{\lambda}{2}\rho\right)P(\zeta)\right]\mathrm{d}\rho\, \mathrm{d}\zeta. \tag{2.8}$$

Kânoğlu & Synolakis (2006) have pointed out that when $u(x, 0) \neq 0$, the initial condition at $t = 0$ does not correspond to an initial condition at $\lambda = 0$. We will not pursue this point here, but note that in the development of detailed rather than idealized solutions to the beach equations this matter may be important (as is the correct handling of incoming boundary data: see Antuono & Brocchini 2007).

To write (2.8) in a form which is slightly more convenient for our purposes, we follow Kânoğlu (2004) by defining

$$\Phi(\zeta) = \frac{1}{\zeta}\frac{\mathrm{d}F}{\mathrm{d}\zeta} \quad \text{and} \quad \Pi(\zeta) = \frac{1}{\zeta}\frac{\mathrm{d}P}{\mathrm{d}\zeta}. \tag{2.9}$$

Assuming that the fluid is initially undisturbed as $x \to \infty$, we may then integrate by parts to write the general solution (2.8) as

$$\phi(\sigma, \lambda) = -\int_0^\infty \int_0^\infty J_0(\rho\sigma) J_1(\rho\zeta)\zeta^2 \left[2\sin\left(\frac{\rho\lambda}{2}\right)\frac{1}{\rho}\Phi(\zeta) + \cos\left(\frac{\rho\lambda}{2}\right)\Pi(\zeta)\right] \mathrm{d}\zeta\,\mathrm{d}\rho, \tag{2.10}$$

where $J_0(x)$ and $J_1(x)$ are standard Bessel functions of the first kind. (Note that (2.10) is exactly equivalent to (2.8), and we do not expect it to have significant advantages over the earlier form of the solution for the purposes of numerical evaluation.)

2.2. *Breakdown of the transformed solutions*

The solutions obtained through the hodograph transformation are valid only while the Jacobian J of the transformation remains positive: if J becomes zero or negative within the solution domain, the solution in the original coordinates becomes multivalued. This is sometimes interpreted as wave breaking, but it is more correct to regard the breakdown of the solutions as a loss of mathematical consistency which anticipates wave breaking, and which necessitates the use of hydrodynamic models that make fewer approximations to the Navier–Stokes equations (e.g. Jensen, Pedersen & Wood 2003; Grilli, Svendsen & Subramanya 1997). Although nonlinear shallow-water theory can predict experimental results surprisingly well even when breakdown does 'just' occur (Synolakis 1987), it has been found to be inadequate for strongly steepening or breaking waves (Jensen *et al.* 2003; Heller, Unger & Hager 2005).

If breakdown occurs the Jacobian could first become zero anywhere in the domain $\sigma \geqslant 0$: it is known, for example, that sufficiently large waves on a sufficiently gentle beach break before reaching the shoreline (see, e.g., Jensen *et al.* 2003), and that any wave of positive amplitude and a positive slope at the wavefront (i.e. a discontinuity in the first spatial derivative of elevation) must break before reaching the shoreline (Greenspan 1958). However, Meyer (1986*a*, *b*) has shown that for smooth initial data, any breakdown within the solution domain must lead to breakdown at the shoreline; and other studies (Carrier & Greenspan 1958; Synolakis 1987; Tinti & Tonini 2005) have found the shoreline value of the Jacobian, $J_{sh}(\lambda)$, to be a good diagnostic of breakdown. (We will comment below on the results of Carrier *et al.* 2003, which appeared to suggest that J_{sh} was not well defined.) When we come to discuss breakdown, we will make the assumption that for the smooth initial conditions we consider, breakdown corresponds simply to the condition that $J_{sh}(\lambda) = 0$ for some $\lambda > 0$.

2.3. *Near-shoreline expansion*

Kânoğlu (2004) obtained the limiting behaviour of the solution (2.10) as $\sigma \to 0$, and thus obtained the shoreline variables $x_{sh}(\lambda)$ and $u_{sh}(\lambda)$. We will extend Kânoğlu's results by obtaining both the leading-order terms in σ and the next-order terms which can be used to approximate the Jacobian just behind the shoreline. To do this, we require the first few terms in the small-σ expansions of all the first and second derivatives of ϕ.

Our starting point is (2.10). We also define some labour-saving quantities,

$$\left.\begin{aligned} S_{2n+1}(\lambda) &\equiv \int_0^\infty \int_0^\infty \zeta^2 J_1(\rho\zeta)\left[\Phi(\zeta)\rho^{2n+1}\sin\left(\frac{\lambda}{2}\rho\right) + \frac{1}{2}\Pi(\zeta)\rho^{2n+2}\cos\left(\frac{\lambda}{2}\rho\right)\right]\mathrm{d}\rho\,\mathrm{d}\zeta, \\ C_{2n}(\lambda) &\equiv \int_0^\infty \int_0^\infty \zeta^2 J_1(\rho\zeta)\left[\Phi(\zeta)\rho^{2n}\cos\left(\frac{\lambda}{2}\rho\right) - \frac{1}{2}\Pi(\zeta)\rho^{2n+1}\sin\left(\frac{\lambda}{2}\rho\right)\right]\mathrm{d}\rho\,\mathrm{d}\zeta, \end{aligned}\right\} \tag{2.11}$$

where $n \in \mathbb{N}$ in each case. We note that

$$\frac{\mathrm{d}C_{2n}}{\mathrm{d}\lambda} = -\frac{1}{2}S_{2n+1}, \quad \frac{\mathrm{d}S_{2n+1}}{\mathrm{d}\lambda} = \frac{1}{2}C_{2(n+1)}, \tag{2.12}$$

and hence

$$S_{2n+1}(\lambda) = (-1)^{n+1}2^{2n+1}\frac{\mathrm{d}^{2n+1}C_0}{\mathrm{d}\lambda^{2n+1}}, \quad C_{2n}(\lambda) = (-1)^n 2^{2n}\frac{\mathrm{d}^{2n}C_0}{\mathrm{d}\lambda^{2n}}. \tag{2.13}$$

It is now simple to expand the various derivatives of $\phi(\sigma, \lambda)$ as power series in σ, obtaining

$$\left.\begin{aligned}
&\frac{\partial\phi}{\partial\lambda} = -C_0 + \frac{C_2}{4}\sigma^2 - \frac{C_4}{64}\sigma^4 + O(\sigma^6), \quad \frac{\partial\phi}{\partial\sigma} = S_1\sigma - \frac{S_3}{8}\sigma^3 + O(\sigma^5),\\
&\frac{\partial^2\phi}{\partial\lambda^2} = \frac{S_1}{2} - \frac{S_3}{8}\sigma^2 + O(\sigma^4), \quad \frac{\partial^2\phi}{\partial\lambda\partial\sigma} = \frac{C_2}{2}\sigma - \frac{C_4}{16}\sigma^3 + O(\sigma^5),\\
&\frac{\partial^2\phi}{\partial\sigma^2} = S_1 - \frac{3S_3}{8}\sigma^2 + O(\sigma^4).
\end{aligned}\right\} \tag{2.14}$$

We thus obtain the shoreline variables u_{sh} and η_{sh}, along with the near-shore expansion for the Jacobian,

$$u_{sh}(\lambda) = -\frac{S_1}{2}, \qquad \eta_{sh} = -x_{sh} = -C_0 - \frac{1}{8}S_1^2 \tag{2.15}$$

and $J \sim J_{sh} + \sigma^2 J_{sh}^{(2)}$, where

$$J_{sh} = \left(1 - \frac{C_2}{4}\right)^2, \quad J_{sh}^{(2)} = \frac{1}{16}\left(1 - \frac{C_2}{4}\right)C_4 - \frac{1}{256}S_3^2. \tag{2.16}$$

We note that the increase of J as $\sigma \to 0$ in figure 17 of Carrier *et al.* (2003) gives a misleading impression, since J tends to a finite limit as $\sigma \to 0$ (cf. Synolakis 1987), rather than growing rapidly in magnitude as the figure suggests.

It is worth considering what the behaviour of the leading-order term $J_{sh}(\lambda)$ tells us about the behaviour of the solution behind the shoreline. $J_{sh}(\lambda)$ is non-negative: as the quantity $1 - C_2/4$ passes through zero, J_{sh} may touch zero briefly but must then increase again. If breakdown occurs at $\lambda = \lambda_c$, so $C_2(\lambda_c) = 4$, then the second-order term will be $J_{sh}^{(2)}(\lambda_c) = -S_3(\lambda_c)^2/256$, which will be negative; hence there will be a small region behind the shoreline in which $J < 0$ and so the solution breaks down. This does not apply, though, in the marginal case when $C_2(\lambda)$ just touches the critical value $C_2 = 4$, so λ_c is a local maximum of $C_2(\lambda)$. In this case, $S_3(\lambda_c) = 0$ from (2.12), and so the second-order term also vanishes: it is straightforward to show that in this case $J \sim C_4^2\sigma^4/1024$, so if the solution only just breaks down at the shoreline, it does not break down behind it.

To evaluate the double integrals $C_{2n}(\lambda)$ and $S_{2n+1}(\lambda)$ efficiently, we again follow Kânoğlu (2004). Employing standard identities (Gradshteyn & Ryzhik 2000, § 6.671), and defining the new time-like variable $\beta = \lambda/2$ for convenience, we can write

$$\int_0^\infty \zeta^2\Phi(\zeta)\left[\int_0^\infty \cos(\beta\rho)J_1(\rho\zeta)\mathrm{d}\rho\right]\mathrm{d}\zeta = \int_0^\infty \zeta\,\Phi(\zeta)\,\mathrm{d}\zeta - \beta^2\Phi(0) - \int_0^1 \beta^3\sqrt{1-z^2}\,\Phi'(\beta z)\,\mathrm{d}z \tag{2.17}$$

and

$$\int_0^\infty \zeta^2 \Pi(\zeta)\left[\int_0^\infty \rho \sin(\beta\rho) J_1(\rho\zeta)\,\mathrm{d}\rho\right]\mathrm{d}\zeta = 2\beta\Pi(0) + \frac{\mathrm{d}}{\mathrm{d}\beta}\int_0^1 \beta^3\sqrt{1-z^2}\,\Pi'(\beta z)\,\mathrm{d}z. \tag{2.18}$$

This enables us to evaluate $C_0(\lambda)$ in terms of single integrals; applying (2.12) repeatedly, we may obtain equivalent expressions for $S_1(\lambda)$, $C_2(\lambda)$ and so forth. All these expressions are readily evaluated using standard routines (the results presented below were obtained using Maple, versions 9 and 10).

3. Gaussian initial waveforms

A particularly tractable set of initial conditions to investigate are the Gaussian waveforms introduced by Carrier *et al.* (2003). These waveforms are defined by the conditions

$$\left.\begin{aligned} P(\zeta) = 0,\ F(\zeta) = a\exp[-k(\zeta^2-1)^2], \\ \text{so } \Phi(\zeta) = -4ka(\zeta^2-1)\exp[-k(\zeta^2-1)^2]. \end{aligned}\right\} \tag{3.1}$$

We have defined the length scale $\hat{L}$ as the offshore position of the centre $\hat{x} = \hat{x}_0$ of the initial waveform, so in terms of Carrier *et al.*'s notation we take $\zeta_0 = 1$. (We note that the toe of the beach should lie somewhat seawards of $x = 1$ so the initial waveform lies almost completely within the sloping region; in the limit as k becomes large, it will suffice if the toe of the beach is an order-unity distance beyond $x = 1$.) The remaining two parameters a and k allow us to vary independently the amplitude and steepness of the initial wave and thus to approximate a variety of smooth localized initial waveforms. In particular, we can take $a > 0$ (a positive Gaussian wave, with initial runup) or $a < 0$ (a negative Gaussian wave, with initial shoreline drawdown). The absolute amplitude of the shoreline motion is proportional to $|a|$ (Kânoğlu 2004), and so we may expect that for sufficiently large positive or negative a the solution will break down. We therefore expect that the solution will remain valid only within a critical range of amplitudes $a_- < a < a_+$, where $a_- < 0$ and $a_+ > 0$.

3.1. *Asymptotics for localized initial waveform*

It is interesting to investigate what happens in the limit as the initial waveform becomes strongly localized, $k \to \infty$. An equivalent limit was investigated by Synolakis (1987) and by Tadepalli & Synolakis (1994), providing useful estimates for the runup height and wave breakdown criterion; as we will see in § 5.1, it may be a particularly relevant regime for some tsunami events.

To do this, we develop asymptotic expressions for C_0, S_1 and C_2 for the Gaussian initial profiles (3.1) in the limit of large k. It is helpful to separate the integrals which contribute to each quantity, writing

$$\left.\begin{aligned} C_0(\beta) &= \int_0^\infty \zeta\,\Phi(\zeta)\,\mathrm{d}\zeta - \beta^2\Phi(0) - I_0(\beta), \quad S_1(\beta) = \frac{1}{2}\beta\Phi(0) + I_1(\beta), \\ C_2(\beta) &= 2\Phi(0) + I_2(\beta), \end{aligned}\right\} \tag{3.2}$$

where

$$\left.\begin{aligned} I_0(\beta) &= \int_0^\beta \beta\sqrt{\beta^2-\zeta^2}\Phi'(\zeta)\,\mathrm{d}\zeta, \quad I_1(\beta) = \int_0^\beta \sqrt{\beta^2-\zeta^2}[3\Phi'(\zeta)+\zeta\Phi''(\zeta)]\,\mathrm{d}\zeta, \\ I_2(\beta) &= \int_0^\beta \frac{\sqrt{\beta^2-\zeta^2}}{\beta}[6(\zeta\Phi'(\zeta))'+\zeta^2\Phi^{(3)}(\zeta)]\,\mathrm{d}\zeta. \end{aligned}\right\} \tag{3.3}$$

From (2.12), we have $I_1 = \mathrm{d}I_0/\mathrm{d}\beta$ and $I_2 = \mathrm{d}^2 I_0/\mathrm{d}\beta^2$; consequently, we need only to evaluate $I_0(\beta)$ to obtain the other terms, as long as the expression for $I_0(\beta)$ is well behaved.

For the initial profile (3.1), with $k \gg 1$, the contributions from the first two terms in C_0 and the first terms in S_1 and C_2 are exponentially small in k, so only the integrals I_0, I_1 and I_2 can contribute significantly to C_0, S_1 and C_2. For this initial profile, we can write the integral I_0 in the form

$$\left.\begin{aligned} I_0(\beta) &= 8ka\beta\int_0^\beta f_0(\zeta)\mathrm{e}^{-kg(\zeta)}\mathrm{d}\zeta, \\ \text{where} \quad g(\zeta) &= (\zeta^2-1)^2 \quad \text{and} \quad f_0(\zeta) = \sqrt{\beta^2-\zeta^2}\zeta[-1+2k(\zeta^2-1)^2]. \end{aligned}\right\} \tag{3.4}$$

The exponential factor in the integrand suggests that when $\zeta = 1$ lies within the range of integration, we should seek a rescaling and expansion about this point, as in the method of steepest descents. Our opportunity to carry out such a rescaling depends on the relative magnitudes of $|\beta-1|$ and k, and so we will investigate three regimes in turn: first the regime $\beta < 1$ and $1-\beta = O(1)$; next the regime $\beta > 1$ and $\beta - 1 = O(1)$; and finally the regime $\beta \approx 1$, more precisely $|1-\beta| = O(k^{-1/2})$.

3.1.1. *The regime* $\beta < 1$ *and* $1-\beta = O(1)$

In the regime $\beta < 1$, $g(\zeta)$ does not have a local minimum within the range of integration; instead, the exponential decays away from the upper limit $\zeta = \beta$. In this case, we apply Watson's lemma, obtaining

$$\begin{aligned} I_0(\beta) &\sim 16\sqrt{2}ak^2\beta^{5/2}(1-\beta^2)^2\mathrm{e}^{-k(\beta^2-1)^2}\int_0^\infty \sqrt{\epsilon}\exp[-4k\beta(\beta^2-1)\epsilon]\mathrm{d}\epsilon \\ &= a\sqrt{2\pi k}\beta(1-\beta^2)^{1/2}\mathrm{e}^{-k(1-\beta^2)^2}. \end{aligned} \tag{3.5}$$

In this regime, then, I_0 and hence C_0 and its derivatives are exponentially small in k. This remains the case as long as the exponent $kg(\zeta)$ remains large, and so we may expect this expansion to break down when $(1-\beta)^2 \sim k$.

3.1.2. *The regime* $\beta > 1$ *and* $\beta - 1 = O(1)$

When $\zeta = 1$ lies within the range of integration, we expect the principal contributions to the integral to come from the region $\zeta - 1 = O(k^{-1/2})$. To capture these contributions, we define a rescaled integration variable $u = (\zeta-1)\sqrt{k}$. We can then write

$$I_0(\beta) = 8k^{1/2}a\beta\int_{-\sqrt{k}}^{(\beta-1)\sqrt{k}} f_0(u)\mathrm{e}^{-kg(u)}\mathrm{d}u, \tag{3.6}$$

where $g(u)$ and $f_0(u)$ are obtained in the obvious manner from $g(\zeta)$ and $f_0(\zeta)$. We now expand the integrand as an asymptotic series in k, obtaining

$$\frac{f_0(u)\mathrm{e}^{-kg(u)}}{\sqrt{\beta^2-1}\mathrm{e}^{-4u^2}} \sim \left(8u^2-1\right) + \left[20u^3-32u^5-u+\frac{u-8u^3}{\beta^2-1}\right]\frac{1}{\sqrt{k}} + \left[(15u^4-80u^6+64u^8)+\frac{\left(\frac{3}{2}u^2+32u^6-24u^4\right)}{\beta^2-1}+\frac{\left(\frac{1}{2}u^2-4u^4\right)}{(\beta^2-1)^2}\right]\frac{1}{k}. \tag{3.7}$$

The leading-order term in this expansion can be written as

$$(8u^2-1)\mathrm{e}^{-4u^2} = -\mathrm{d}(u\mathrm{e}^{-4u^2})/\mathrm{d}u,$$

and so when it is integrated between $-\sqrt{k}$ and $(\beta-1)\sqrt{k}$ the contributions it makes are exponentially small in k. At the next order, all the terms of $O(k^{-1/2})$ are odd in u, so when we integrate this term over the required range, we have complete cancellation in the region where the integrand is relatively large, and the contributions are again exponentially small in k.

It is only at the next order in k that we find a term which does not make an exponentially small contribution to I_0. Evaluating the corresponding integral, we obtain

$$I_0(\beta) \sim -\frac{a\sqrt{\pi}}{4\sqrt{k}}\frac{\beta}{(\beta^2-1)^{3/2}}\left[\mathrm{erf}(2\sqrt{k})+\mathrm{erf}(2(\beta-1)\sqrt{k})\right] \sim -\frac{a\sqrt{\pi}}{2\sqrt{k}}\frac{\beta}{(\beta^2-1)^{3/2}}.$$

We can obtain $I_1(\beta)$ and $I_2(\beta)$ either by an equivalent expansion or directly from $I_0(\beta)$:

$$\left.\begin{aligned} I_1(\beta) &\sim \frac{\mathrm{d}}{\mathrm{d}\beta}\left(-\frac{a\sqrt{\pi}}{2\sqrt{k}}\frac{\beta}{(\beta^2-1)^{3/2}}\right) = \frac{\sqrt{\pi}}{2\sqrt{k}}a\frac{2\beta^2+1}{(\beta^2-1)^{5/2}}, \\ I_2(\beta) &\sim \frac{\mathrm{d}^2}{\mathrm{d}\beta^2}\left(-\frac{a\sqrt{\pi}}{2\sqrt{k}}\frac{\beta}{(\beta^2-1)^{3/2}}\right) = -\frac{3\sqrt{\pi}}{2\sqrt{k}}a\frac{\beta(2\beta^2+3)}{(\beta^2-1)^{7/2}}. \end{aligned}\right\} \tag{3.8}$$

Note that these terms are proportional to $a/\sqrt{k}$ and thus to the volume of the initial waveform: this is to be expected, since they represent the relaxation of the shoreline towards rest at large times, and so are sensitive not to the shape of the wave but to its magnitude.

3.1.3. *The regime* $|\beta-1| = O(k^{-1/2})$

Finally, we consider the regime $|\beta-1| = O(k^{-1/2})$. To investigate this regime, we define two rescaled variables: $u = (\zeta-1)\sqrt{k}$ as before, and $b = 2(\beta-1)\sqrt{k}$. We can now write

$$I_0 = 8k^{1/2}a\beta\int_{-\sqrt{k}}^{b/2} f_0(u)\mathrm{e}^{-kg(u)}\mathrm{d}u, \tag{3.9}$$

where $f_0(u)$ and $g(u)$ are defined as before. Expanding the integrand and taking only the leading-order term, we obtain

$$I_0 = 8\sqrt{2}ak^{1/4}\int_{-\sqrt{k}}^{b/2}\left(\frac{b}{2}-u\right)^{1/2}(-1+8u^2)\mathrm{e}^{-4u^2}\mathrm{d}u + O(k^{-1/4}). \tag{3.10}$$

Neglecting exponentially small terms in k, we may let the lower limit tend to infinity; we then make the further change of integration variable to $w = b - 2u$, obtaining

$$I_0 \sim 4ak^{1/4} Z(b), \quad \text{where} \quad Z(b) = \int_0^\infty \sqrt{w}(-1 + 2(b-w)^2) \mathrm{e}^{-(b-w)^2} \mathrm{d}w. \tag{3.11}$$

Similarly, we may obtain $I_1 \sim 8ak^{3/4} Z'(b)$ and $I_2 \sim 16ak^{5/4} Z''(b)$. With some manipulation, $Z(b)$ and its derivatives can be expressed in terms of standard functions, but it is simpler to use them directly. We are interested in particular in the global minimum and maximum of $Z(b)$ (which controls runup and rundown), of $Z'(b)$ (which controls shoreline velocity), and of $Z''(b)$ (which controls the Jacobian). It is simple to establish that the global maximum of Z is given approximately by $Z(-0.3895) \approx 0.3981$, while the global minimum of Z is given approximately by $Z(1.235) \approx -0.1830$. The global maximum of Z' is given approximately by $Z'(-0.9810) \approx 0.3803$, and the global minimum by $Z'(0.3194) \approx -0.6066$; while the global minimum of Z'' is given approximately by $Z''(-0.2771) \approx -1.2479$, and the global maximum by $Z''(0.8421) \approx 0.8916$.

Finally, we can use these data to estimate the maximum and minimum values of C_0, S_1 and C_2 in this asymptotic limit: we have (remembering that $C_0 \sim -I_0$, and assuming $a > 0$)

$$-1.5926ak^{1/4} = C_0^{min} \lesssim C_0 \lesssim C_0^{max} = 0.7318ak^{1/4}, \tag{3.12}$$

$$-4.8527ak^{3/4} = S_1^{min} \lesssim S_1 \lesssim S_1^{max} = 3.0425ak^{3/4}, \tag{3.13}$$

$$-19.966ak^{5/4} = C_2^{min} \lesssim C_2 \lesssim C_2^{max} = 14.26ak^{5/4}. \tag{3.14}$$

Crucially, the estimates obtained here for C_0, S_1 and C_2 are asymptotically larger than those in either of the regimes where $|\beta - 1| \gg k^{-1/2}$, and we deduce that these are estimates for the global maxima and minima of these quantities when $k \gg 1$. We will use these results to collapse the data from a full treatment of the shoreline hydrodynamics, and then discuss some further applications.

3.2. *Convergence to the asymptotic solution*

Having derived the asymptotic representation of a 'pulse-like' wave in the limit of large k, it is natural to ask how well it approximates the shoreline motion for initial waveforms with a finite value of k. We will consider first the description of the shoreline position $x_{sh}(\beta)$, and then the description of the shoreline Jacobian $J_{sh}(\beta)$.

3.2.1. *Shoreline motion*

Figure 1 illustrates the shoreline motion for a range of values of a and k, and compares the full solutions for x_{sh} with the 'pulse-like' estimates $x_{sh} \sim -4ak^{1/4} Z(b) + 8a^2 k^{3/2} [Z'(b)]^2$.

Figures 1(a) and 1(b) show the convergence towards the asymptotic solution as k increases while keeping a fixed. Although the maximum and minimum of x_{sh}, which occur when $S_1 = 0$, scale with $k^{1/4}$, the shape of the asymptotic solution changes somewhat with k as the relative importance of the $Z'(b)$ and $Z(b)$ terms changes; consequently, as k increases the shoreline accelerates more and more strongly, and ultimately the solution breaks down. (This will be discussed in the next section; for the moment we note from figure 1b that the difference between the scaled asymptotic predictions for $k = 1$ and $k = 16$ is not very great.) For $a = 0.005$, this breakdown occurs around $k = 20$; as these figures indicate, though, below this value of k the asymptotic estimates are reasonably good; in fact, they are only inaccurate by a factor of order unity even for $k = 1$.

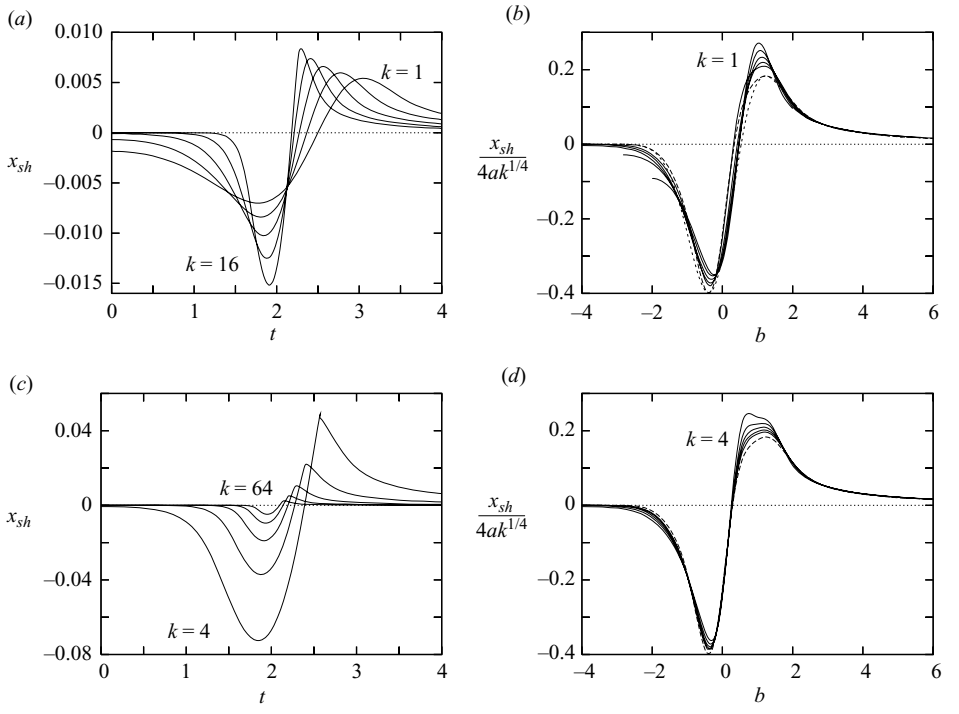

FIGURE 1. Shoreline motion under Gaussian initial waveforms, compared with large-k asymptotic estimates. (a), (b) Amplitude $a = 0.005$ and $k = 1$ to 16: (a) shows the unscaled shoreline position $x_{sh}(t)$, while (b) shows the scaled shoreline position $x_{sh}/(4ak^{1/4})$ (solid lines) for the same values of a and k, compared with the asymptotic estimate plotted for $a = 0.005$ and $k = 1$ (heavy dashed lines), $k = 16$ (light dashed lines). (c), (d) Amplitude $a = 0.2k^{-5/4}$ and $k = 4$ to 64: (c) shows the unscaled shoreline position $x_{sh}(t)$, while (d) shows the scaled shoreline position $x_{sh}/(4ak^{1/4})$ (solid lines) for the same values of a and k, compared with the asymptotic estimate for $ak^{5/4} = 0.2$ (dashed line).

Figures 1(c) and (d) show the convergence towards the asymptotic solution when we decrease a with increasing k, keeping $ak^{5/4}$ fixed. This ensures that the relative importances of the $Z(b)$ and $Z'(b)$ terms in the asymptotic solution are the same for all values of k, so the rescaled shoreline positions should collapse towards a single curve (the dashed line in figure 1d). A consequence of this is that we guarantee that the solution does not break down with increasing k (although breakdown can be seen in figure 1c for the curve $k = 4$ at around $t = 2.6$). The convergence in figure 1(d) is clear, and again the asymptotic solution provides a reasonable approximation for k of order unity, even though convergence is formally rather slow: the correction term in (3.10) decays only as $k^{-1/4}$.

In general, the asymptotic solution for the shoreline accelerates later than the finite-k shoreline, due to the neglect of contributions from the region $\beta < 1$ and $|1 - \beta| = O(1)$, and it overestimates the initial excursion of the shoreline; correspondingly, it underestimates the second excursion of the shoreline. Overall, however, the comparison supports the use of the asymptotic solution as an approximation to shoreline motion under waves with finite k.

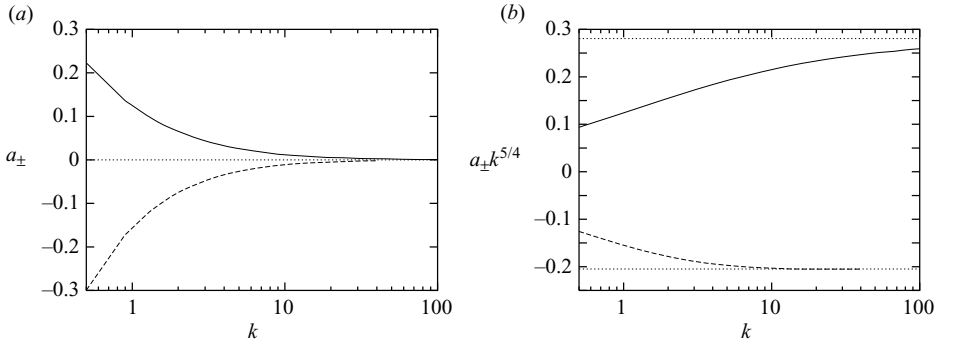

FIGURE 2. Critical amplitudes $a_\pm$ for the shoreline breakdown of an initially Gaussian wave: (*a*) original amplitudes; (*b*) amplitudes scaled by the asymptotic factor $k^{-5/4}$.

3.2.2. *The behaviour of the Jacobian and solution breakdown*

We now investigate the criterion for breakdown of the shoreline solutions for finite k, evaluating the integral (2.11) for $C_2(\beta)$ numerically using the adaptive integration routines in Maple 10. The critical condition on the amplitude may be written as $1-\frac{1}{4}C_2(\beta_{crit})=0$ for some $\beta_{crit}>0$, while $1-\frac{1}{4}C_2(\beta)>0$ for all other values of β. We can use the linearity of C_2 to write

$$C_2(\beta)=aC_2^{a=1}(\beta), \quad \text{where} \quad C_2^{a=1}(\beta)=[2\Phi(0;a=1)+I_2(\beta;a=1)]\,. \tag{3.15}$$

Here I_2 is defined in (3.3), and we define $C_2^{a=1}(\beta)$ for notational convenience below. Since $C_2^{a=1}(\beta)$ can be either positive or negative, the two critical values of a correspond to

$$a_-=4\big[\min_\beta C_2^{a=1}(\beta)\big]^{-1}, \qquad a_+=4\big[\max_\beta C_2^{a=1}(\beta)\big]^{-1}. \tag{3.16}$$

It is reasonably straightforward to locate numerically the global maximum and minimum of $I_2(\beta)$ over β for a given k, and thus to calculate $a_\pm$. We also recall that in the limit of large k, we expect that $\max_\beta C_2^{a=1}\approx 14.26k^{5/4}$ and $\min_\beta C_2^{a=1}\approx -19.966k^{5/4}$, and hence $a_+\simeq 0.280k^{-5/4}$ and $a_-\simeq -0.200k^{-5/4}$.

Figure 2 shows the results for $a_\pm$ across a range of k. The magnitudes of $a_\pm$ decrease as k increases (figure 2*a*), since a steeper initial wave has more chance of breaking. Even for quite moderate values of k, the amplitudes required for the solution not to break down may be rather small (of the order of 10^{-3} and less). As figure 2(*b*) demonstrates, the asymptotic result $k^{5/4}a_\pm\sim$ constant describes rather well how the critical amplitude varies: even for $k=1$, it only overestimates the critical amplitude by roughly a factor of 2, and it becomes increasingly accurate as k increases. (The convergence is somewhat faster for a_-, i.e. a negative initial Gaussian.) From our numerical results, $a_+\approx 0.28k^{-5/4}$, while $a_-\approx -0.205k^{-5/4}$, which compares extremely well with the asymptotic estimates. We further note from (3.12) that since the shoreline excursion is given asymptotically by $(C_0^{max}-C_0^{min})\approx 2.3244|a|k^{1/4}$, we can relate the maximum shoreline excursion E of a shallow-water solution to its source conditions by $E\sim 2.3244a_+k^{1/4}\approx 0.653/k$ for $a>0$, and $E\sim 2.3244|a_-|k^{1/4}\approx 0.465/k$ for $a<0$. This suggests that nonlinear shallow-water theory can be used to describe results with significant shoreline motion only when their source is rather close to the shore or not strongly spatially localized; we will see in § 5.1, however, that this does not preclude its use for descriptions of tsunami runup.

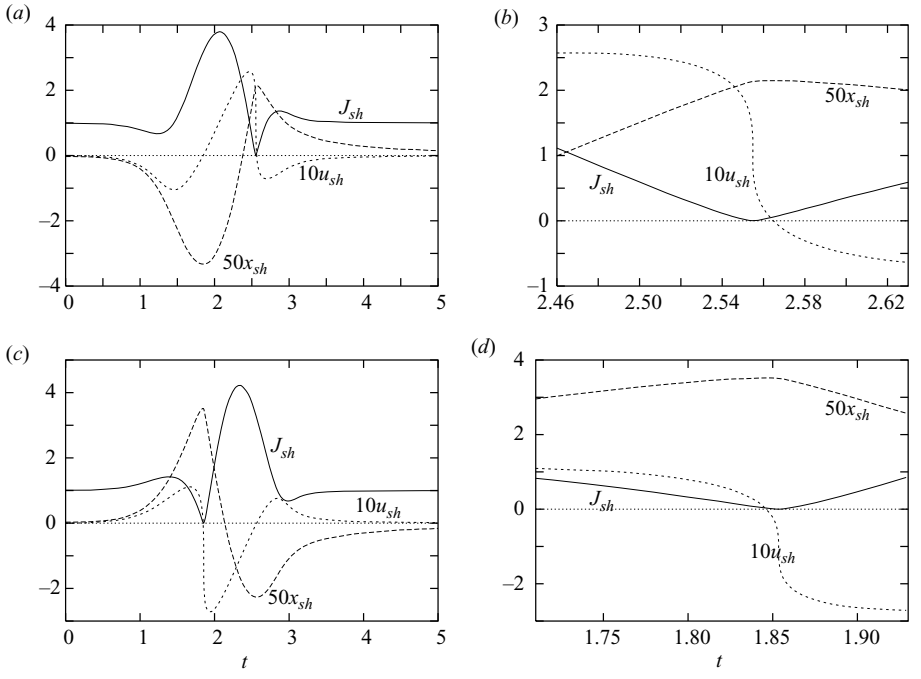

FIGURE 3. Shoreline quantities $J_{sh}(t)$, $x_{sh}(t)$ and $u_{sh}(t)$ for the case $k=4$ and (a, b) $a=a_+ \approx 0.0325$; (c, d) $a=a_- \approx -0.0343$. Figures (b) and (d) are enlargements of figures (a) and (c) respectively about the point of maximum run-down: note that $u_{sh}(\lambda_+)>0$ and $u_{sh}(\lambda_-)<0$.

Figure 3 illustrates the shoreline hydrodynamics for the critical cases when $a=a_\pm$. For both positive and negative Gaussian critical solutions, the breakdown of the solution occurs very close to the point of maximum rundown (from § 3.1.3, we expect the value of β at breakdown to be within $O(k^{-1/2})$ of $\beta=1$). For a positive Gaussian (figure 3*b*), breakdown occurs on the backwash $u_{sh}>0$, very slightly before maximum rundown; for a negative Gaussian (figure 3*d*), it occurs on the runup $u_{sh}<0$, very slightly after maximum rundown. Since a positive Gaussian has to run up before running down while the first shoreline motion for a negative Gaussian is rundown, the negative critical solution breaks down sooner than the positive one: this corresponds to the fact that in the limit $k \to 0$ the minimum of C_2 for $a>0$ always occurs before the maximum.

Finally, we note in passing that we have also carried out a short series of numerical experiments, using the implementation of Carrier *et al.*'s (2003) solution described by Dickinson (2005), in which a was varied beyond the range $a_- < a < a_+$ for various k; in each case breakdown of the solution occurred most readily at the shoreline, supporting our use of J_{sh} as a diagnostic of breakdown. We omit the details of these computations here as they lie outwith the main topic of the current study.

3.3. *Shoreline forces and their effects*

As well as using our asymptotic results for pulse-like Gaussian waves to investigate runup and solution breakdown, it is interesting to obtain predictions for the ability of waves to mobilise or damage sediment or larger objects in their path. Quantifying this ability is particularly important in hazard assessment, both when assessing the likely

impact of waves on coasts and when interpreting the traces they leave (Dawson & Shi 2000; Nott 2003). A preliminary analysis was made by Carrier *et al.* (2003) by considering the momentum flux under the wave: this describes the forces applied to objects which occupy the full depth of the flow, and their results have recently been extended through numerical computations by Yeh (2006). We can extend these ideas to immersed objects with only a little effort.

In broad terms, objects immersed in a flow are subjected to two types of mobilizing forces: turbulent drag or lift forces and forces due to pressure gradients. (The latter have traditionally been considered insignificant for sediment, but there is increasing interest in their role in coastal settings: see, e.g., Hoefel & Elgar 2003.) For a body with characteristic length scale $\hat{D}$ (and corresponding surface area $\hat{D}^2$), we may estimate the net forces exerted by turbulent drag and the pressure gradient as, respectively,

$$\hat{F}_d \approx \hat{\tau}_d \hat{D}^2 = c_d \hat{\rho} \bar{u}^2 \hat{D}^2, \quad \hat{F}_p \approx \left| \frac{\partial \hat{p}}{\partial \hat{x}} \right| \hat{D}^3 = \hat{g} \hat{\rho} \left| \frac{\partial \hat{\eta}}{\partial \hat{x}} \right| \hat{D}^3, \tag{3.17}$$

where c_d is a dimensionless Chezy drag coefficient, $\hat{\rho}$ the fluid density and $\hat{p}$ the fluid pressure. The drag coefficient c_d is typically small, of order 10^{-3}–10^{-2}, for the bottom friction which mobilizes sediment (Dyer 1986), but can be of order unity when evaluating the form drag and the lift associated with flow around a large body (Luccio *et al.* 1998; Yeh 2006). We note that Nott (2003) has provided more detailed estimates of boulder mobilization based on the moments exerted on asymmetrical bodies, but with a simpler description of the hydrodynamics. Luccio *et al.* (1998) have also provided and validated experimentally a detailed model of cobble transport under swash flow with ballistic shoreline motion: although their model is not directly applicable to transport under a (non-breaking) tsunami, the physical assumptions underlying it are essentially the same as those employed here.

We can write $\hat{F}_d$ and $\hat{F}_p$ in terms of the hodograph-transformed variables as

$$\hat{F}_d \approx [c_d \hat{\rho} \hat{D}^2 \hat{g} \hat{L} \tan\alpha] u^2 = [c_d \hat{\rho} \hat{D}^2 \hat{g} \hat{L} \tan\alpha] \left(\frac{1}{2\sigma} \frac{\partial \phi}{\partial \sigma} \right)^2, \tag{3.18}$$

$$\hat{F}_p \approx [\hat{g} \hat{\rho} \hat{D}^3 \tan\alpha] \frac{\partial \eta}{\partial x} = [\hat{g} \hat{\rho} \hat{D}^3 \tan\alpha] \left| \frac{1}{J} \frac{\partial t}{\partial \lambda} - 1 \right| = [\hat{g} \hat{\rho} \hat{D}^3 \tan\alpha] \left| \frac{1}{J} - 1 - \frac{1}{2\sigma J} \frac{\partial^2 \phi}{\partial \sigma \partial \lambda} \right|. \tag{3.19}$$

This expression for $\hat{F}_p$ will grow unboundedly as the wave steepens towards breakdown, and so we will restrict our estimates to the regime where $J = O(1)$.

Our asymptotic results supply estimates of the magnitudes of $\hat{F}_d$ and $\hat{F}_p$ in terms of the source of an incoming wave. As before, we assume that the extrema of all hydrodynamic quantities occur at or near the shoreline, and that the incoming waveform is relatively localized.

Assuming that the incoming wave is a Gaussian of the form (3.1), we may use the near-shoreline estimates

$$u \sim -\frac{1}{2} S_1(\lambda) \sim 4ak^{3/4} Z'(b), \quad \frac{\partial^2 \phi}{\partial \lambda \partial \sigma} \sim \frac{1}{2} \sigma C_2(\lambda) \sim 8\sigma a k^{5/4} Z''(b) \tag{3.20}$$

to obtain

$$\hat{F}_d \approx c_d \hat{\rho} \hat{g} \hat{D}^2 \hat{L} \tan\alpha \frac{S_1^2}{4}, \quad \hat{F}_p \approx \hat{\rho} \hat{g} \hat{D}^3 \tan\alpha \left| \frac{C_2}{4 - C_2} \right|. \tag{3.21}$$

If the wave is some way from breaking, we can approximate the final term in $\hat{F}_d$ simply as $C_2/4$, and then use (3.13) and (3.14) to obtain

$$\left.\begin{aligned} \max|\hat{F}_d| &\approx \left[\frac{c_d}{4}\hat{\rho}\hat{g}\hat{D}^2\hat{L}\tan\alpha\right]\max_{\lambda} S_1^2(\lambda) = 5.887[c_d\hat{\rho}\hat{g}\hat{D}^2\hat{L}\tan\alpha](ak^{3/4})^2, \\ \max|\hat{F}_p| &\approx [\hat{\rho}\hat{g}\hat{D}^3\tan\alpha]\max_{\lambda}|C_2(\lambda)| = 19.97[\hat{\rho}\hat{g}\hat{D}^3\tan\alpha]ak^{5/4}. \end{aligned}\right\} \tag{3.22}$$

We will apply these estimates in § 5.1.2 to consider the impact of a particular tsunami event.

3.4. *Non-zero initial velocities*

Our calculations so far have been carried out assuming that the initial condition is one in which surface elevation is disturbed without a corresponding disturbance to velocity. This is a good approximation to reality only if the initial waveform is generated very rapidly: for example, by a seismic event in which the fault displacement velocity is much greater than the local water wave celerity. In general, it is necessary to consider the effects of an initial velocity field.

In principle, the initial velocity and elevation fields can be specified independently, but it is convenient to consider them to be closely related. The standard assumption (see, e.g., Carrier *et al.* 2003; Kânoğlu & Synolakis 2006) is that the velocity field is that for a deep-water wave propagating onshore, so $u(x,0) = -(2\sqrt{x+\eta(x,0)} - 2\sqrt{x})$ or, with a further approximation, $u(x,0) = -\eta(x,0)/\sqrt{x}$. For our purposes, the first expression is rather cumbersome, while the second introduces a singularity in the initial velocity as $x \to 0$ unless $\eta(0,0) = 0$; this singularity can be eliminated numerically, but would disrupt the asymptotic expansion we wish to carry out for a localized waveform. We will therefore employ a further simplification appropriate for a localized initial condition, which is to set simply $u(x,0) = -\eta(x,0)$, so the wave celerity is that appropriate to the centre of the initial waveform. This removes the shoreline singularity and makes the asymptotics relatively straightforward, although it introduces some error if we consider that velocity should be specified exactly using the standard assumption. Certainly for detailed simulations the approach of Kânoğlu & Synolakis (2006) for the initial value problem, or the incoming-characteristic specification of Antuono & Brocchini (2007) for the boundary-value problem, would be more appropriate to adopt. For reasons of analytical tractability, we do not consider here these more correct formulations: it appears likely that their general forms for the solution could be approximated asymptotically in the same way as the solutions of Carrier *et al.* (2003), but this lies beyond the scope of the current study.

Taking the Gaussian initial elevation described above, we have

$$\eta(x,0) = a\exp[-k(x-1)^2], \quad u(x,0) = -a\exp[-k(x-1)^2], \tag{3.23}$$

giving, with the usual approximation $x = \sigma^2$ at $\lambda = 0$,

$$F(\sigma) = a\exp[-k(\sigma^2-1)^2] + \frac{1}{2}a^2\exp[-2k(\sigma^2-1)^2], \tag{3.24}$$

$$P(\sigma) = \int_0^{\sigma} 2\sigma' a\exp[-k(\sigma'^2-1)^2]\,\mathrm{d}\sigma', \tag{3.25}$$

and thus

$$\Phi(\zeta) = -4ka(\zeta^2-1)\exp[-k(\zeta^2-1)^2] - 4ka^2(\zeta^2-1)\exp[-2k(\zeta^2-1)^2], \tag{3.26}$$

$$\Pi(\zeta) = 2a\exp[-k(\zeta^2-1)^2]. \tag{3.27}$$

We require to calculate an asymptotic representation of $C_0(\beta)$; as before, all other results will follow from this. Echoing § 3.1, we may write (2.17) and (2.18) as

$$\int_0^\infty \zeta^2 \Phi(\zeta) \left[\int_0^\infty \cos(\beta\rho)\, J_1(\rho\zeta)\, \mathrm{d}\rho \right] \mathrm{d}\zeta = \int_0^\infty \zeta \Phi(\zeta)\, \mathrm{d}\zeta - \beta^2 \Phi(0) - I_0(\beta), \quad (3.28)$$

$$\int_0^\infty \zeta^2 \Pi(\zeta) \left[\int_0^\infty \rho \sin(\beta\rho)\, J_1(\rho\zeta)\, \mathrm{d}\rho \right] \mathrm{d}\zeta = 2\beta\Pi(0) + H_0(\beta), \quad (3.29)$$

where

$$I_0(\beta) = \int_0^1 \beta^3 \sqrt{1-z^2}\, \Phi'(\beta z)\, \mathrm{d}z, \quad H_0(\beta) = \frac{\mathrm{d}}{\mathrm{d}\beta} \int_0^1 \beta^3 \sqrt{1-z^2}\, \Pi'(\beta z)\, \mathrm{d}z. \quad (3.30)$$

The two terms which contribute to $\Phi(\zeta)$, and thus to $I_0(\beta)$, are very similar in form, and it is simple to adapt the analysis in § 3.1 to show that

$$I_0(\beta) \sim 4ak^{1/4} Z(b) + 2^{5/4} a^2 k^{1/4} Z(b\sqrt{2}), \quad (3.31)$$

where Z is defined in (3.11).

Evaluating $H_0(\beta)$ requires only a little more effort. We may easily obtain

$$\Pi'(\zeta) = -8ak\zeta(\zeta^2-1)\exp[-k(\zeta^2-1)^2], \quad (3.32)$$

$$\Pi''(\zeta) = -8ak \exp[-k(\zeta^2-1)^2]\{3\zeta^2 - 4k\zeta^2(\zeta^2-1)^2 - 1\}, \quad (3.33)$$

and hence

$$H_0(\beta) = \int_0^1 [2\beta^2 \sqrt{1-z^2}\, \Pi'(\beta z) + \beta^3 \sqrt{1-z^2} z \Pi''(\beta z)]\, \mathrm{d}z$$

$$= 8ak \int_0^\beta \sqrt{\beta^2 - \zeta^2} \mathrm{e}^{-k(\zeta^2-1)^2} \zeta \left\{ -5\zeta^2 + 3 + 4k\zeta^2(\zeta^2-1)^2 \right\} \mathrm{d}\zeta. \quad (3.34)$$

We now make the same substitutions as before, defining $b = 2(\beta-1)\sqrt{k}$ and $u = (\zeta-1)\sqrt{k}$. Concentrating our attention on the regime $|\beta - 1| = O(k^{-1/2})$, it follows by expanding the integrand as a series in $1/k$ that

$$H_0(\beta) \sim 8ak 2^{3/2} k^{-3/4} \int_{-\sqrt{k}}^{b/2} \left(\frac{b}{2} - u \right)^{1/2} (-1 + 8u^2) \mathrm{e}^{-4u^2} \mathrm{d}u \quad (3.35)$$

$$\sim 8ak^{1/4} Z(b), \quad (3.36)$$

where $Z(b)$ is defined exactly as before (see (3.10)).

Putting these results together using (2.11), we have

$$C_0(\beta) \sim -I_0(\beta) - \tfrac{1}{2} H_0(\beta) \sim -8ak^{1/4} Z(b) - 2^{5/4} a^2 k^{1/4} Z(b\sqrt{2}). \quad (3.37)$$

In the regime $a \ll 1$ where the second term may be neglected, this result indicates that by including an initial velocity calculated according to the usual assumption, we amplify all extremal quantities associated with the shoreline motion by a factor of 2. This solution will break down for initial amplitudes which are only a half of the critical values calculated in § 3.2; if it does not break down then the shoreline excursion and maximum velocities will be twice as large as those calculated in § 3.2. This result might be anticipated physically, as including an initial velocity in this manner ensures that the initial wave is entirely incoming (to a first approximation), rather than splitting into incoming and outgoing waves as does the zero-velocity initial wave (see figures 5 and 8 of Carrier *et al.* 2003). It underlines the importance

of accurately representing the 'initial' velocity of an incoming wave when forecasting the effects of tsunamis.

4. Other initial waveforms: Carrier *et al.*'s N-waves

The Gaussian initial waveform considered by Carrier *et al.* (2003) is relatively simple; however, we can readily use the linearity of the shoreline quantities C_n and S_n in Φ to construct solutions for rather more complicated initial conditions by superimposing Gaussians of different shapes, sizes and positions. In particular, Carrier *et al.* (2003) constructed various N-waves, similar but not identical to those introduced to tsunami studies by Tadepalli & Synolakis (1994), by summing two Gaussians of opposite sign. We can investigate the 'pulse-like' limit of these N-waves in the same way as we investigated this limit for Gaussian waves, with only a minor additional algebraic effort.

The double-Gaussian N-wave has initial condition

$$F(\zeta) = a\exp[-k(\zeta^2-1)^2] + a_2\exp\left[-k_2\left(\zeta^2-\zeta_2^2\right)^2\right], \tag{4.1}$$

where $\zeta_2 > 1$, and where for an N-wave we must have $aa_2 < 0$. This gives

$$\Phi(\zeta) = -4ka(\zeta^2-1)\exp[-k(\zeta^2-1)^2] - 4k_2a_2\left(\zeta^2-\zeta_2^2\right)\exp\left[-k_2\left(\zeta^2-\zeta_2^2\right)^2\right]. \tag{4.2}$$

The limit of a localized waveform will be most interesting if the two Gaussians narrow at the same rate and if the distance between them shrinks similarly, so the waveforms do not simply become two non-interacting Gaussian waves. We will confine ourselves to considering this distinguished limit: in other words, we take $k_2 = \kappa_2 k$ and $\zeta_2 = 1 + k^{-1/2}\Delta$, where κ_2 and Δ are of order unity, and we consider the limit $k \to \infty$ as before.

We can write $C_0(\beta)$ in terms of $I_0(\beta)$ and exponentially small contributions as before, and furthermore write I_0 as the sum of the contributions from the two Gaussians: $I_0(\beta) = I_0^{(1)}(\beta) + I_0^{(2)}(\beta)$, where $I_0^{(1)}$ is identical to the expression (3.11) obtained above and where

$$\begin{aligned} I_0^{(2)}(\beta) &= 8k_2a_2\beta\int_0^\beta \sqrt{\beta^2-\zeta^2}\zeta\left[-1+2k_2\left(\zeta^2-\zeta_2^2\right)^2\right]\exp\left[-k_2(\zeta^2-\zeta_2^2)^2\right]\mathrm{d}\zeta \\ &= 8K_2a_2B\int_0^B \sqrt{B^2-z^2}z[-1+2K_2(z^2-1)^2]\exp[-K_2(z^2-1)^2]\mathrm{d}z, \end{aligned} \tag{4.3}$$

where we have defined $B = \beta/\zeta_2$ and $K_2 = k_2\zeta_2^4$. (It is not surprising that we can scale out ζ_2 in this way, given the indeterminacy of the length scale $\hat{L}$ in the non-dimensionalisation of the governing equations: see § 2.1.) The asymptotics of $I_0^{(2)}$ follow exactly as in § 3.1, and we obtain

$$I_0^{(2)}(\beta) \sim 4a_2K_2^{1/4}Z(b_2), \qquad \text{where} \qquad b_2 = 2(B-1)\sqrt{K_2}. \tag{4.4}$$

Writing the two terms using the same variables, we find

$$\begin{aligned} b_2 &= 2\left(\frac{\beta}{\zeta_2}-1\right)\sqrt{k_2}\zeta_2^2 = 2\left(1+\frac{\Delta}{k^{1/2}}\right)\sqrt{k_2}\left(\frac{b}{2k^{1/2}}-\frac{\Delta}{k^{1/2}}\right) \\ &= 2\kappa_2^{1/2}\left(1+\frac{\Delta}{k^{1/2}}\right)\left(\frac{b}{2}-\Delta\right), \end{aligned} \tag{4.5}$$

$$I_0^{(2)}(\beta) \sim 4a_2\zeta_2k_2^{1/4}Z(b_2) = 4a_2\left(1+\frac{\Delta}{k^{1/2}}\right)k^{1/4}\kappa_2^{1/4}Z(b_2); \tag{4.6}$$

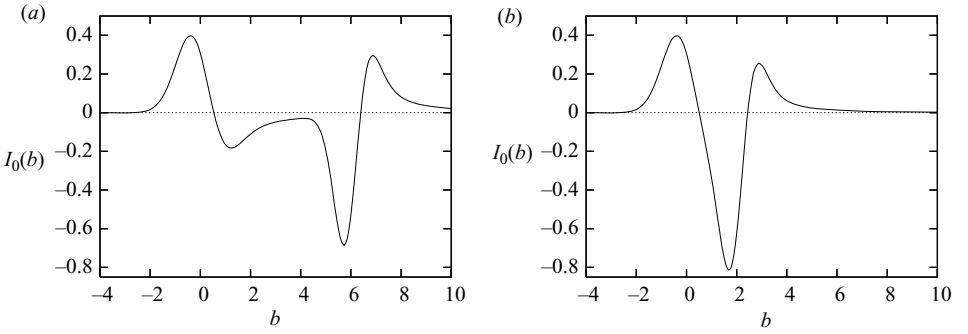

FIGURE 4. Asymptotic estimate for the shoreline elevation, $\eta_{sh}(\lambda) \sim I_0(b)$, under landslide-generated N-waves with (*a*) $\kappa_2 = 2$ and $\Delta = 3$, (*b*) $\kappa_2 = 2$ and $\Delta = 1$.

and thus, writing $A_2 = a_2/a < 0$,

$$I_0(\beta) \sim 4ak^{1/4}\left[Z(b) + A_2\kappa_2^{1/4}\left(1+\frac{\Delta}{k^{1/2}}\right)Z\left(2\kappa_2^{1/2}\left(1+\frac{\Delta}{k^{1/2}}\right)\left(\frac{b}{2}-\Delta\right)\right)\right] \tag{4.7}$$

$$\sim 4ak^{1/4}\left[Z(b) + A_2\kappa_2^{1/4}Z\left(2\kappa_2^{1/2}\left(\frac{b}{2}-\Delta\right)\right)\right] \tag{4.8}$$

$$\equiv 4ak^{1/4}Z_N(b), \tag{4.9}$$

where we have defined the quantity $Z_N(b)$ for convenience later. In a similar way, we have $I_1(\beta) \sim 8ak^{3/4}Z_N'(b)$ and $I_2(\beta) \sim 16ak^{5/4}Z_N''(b)$.

Before proceeding, we note that it is relatively straightforward, using the above approach, to determine an asymptotically valid description of the shoreline hydrodynamics for a localized initial condition consisting of several superimposed Gaussian waveforms. While we will not pursue this possibility here, we note it as a potentially useful tool for future investigations of how initial conditions control wave runup.

4.1. *Extremal behaviour of landslide-generated N-waves*

As an application, we consider the extrema of shoreline position and the solution breakdown condition predicted by (4.9). This expression contains, as well as the parameters a and k, the additional parameters A_2, κ_2 and Δ, which together control the shape of the initial N-wave. To avoid having to consider a three-dimensional parameter space, we will restrict ourselves here to initial waveforms, such as example (*d*) of Carrier *et al.* (2003), that conserve the mass of water and represent waves generated by a submarine landslide or similar displacement. These satisfy the additional condition that $A_2 = -\kappa_2^{1/2}$, leaving us with two parameters to vary.

Figure 4 illustrates the shoreline motion under two N-waves with slightly different parameters, assuming $a > 0$ (a leading-elevation N-wave). Recall that the 'N-wave' comprises a leading positive Gaussian centred at $\zeta = 1$ and with amplitude a and width $k^{-1/2}$, followed by a negative Gaussian centred at $\zeta_2 = 1 + \Delta k^{-1/2}$ and with amplitude $a\sqrt{\kappa_2}$ and width $(k\kappa_2)^{-1/2}$. If the two waves are widely spaced (large values of Δ) their contributions to shoreline motions are effectively separate: the leading wave produces runup followed by backwash and then recovery towards mean sea level; the following wave then arrives, causing drawdown followed by runup and gradual retreat (figure 4*a*). In this limit, an extremum of shoreline position will clearly be an extremum of one wave or the other; which it is will depend on the values of κ_2 and Δ. For lower values of Δ, the backwash of the leading wave and the drawdown

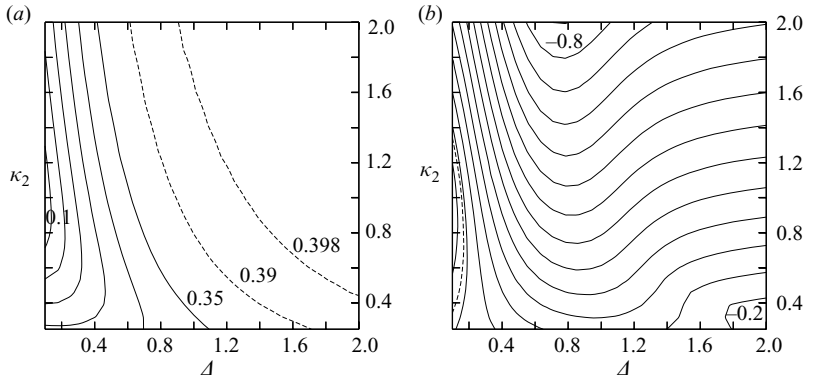

FIGURE 5. Extrema of the asymptotic forms for $I_0(b)$ for landslide-generated N-waves. (a) The maximum over b of $Z_N(b) = I_0(b)/(4ak^{1/4})$: dashed lines are contours at 0.39 and 0.398; solid lines are contours at 0.1 to 0.35 by 0.05. (b) The minimum over b of $Z_N(b) = I_0(b)/(4ak^{1/4})$: the dashed line is the contour at -0.183; solid lines are contours at -0.15 to -0.8 by -0.05.

of the following wave combine constructively, increasing the maximum drawdown (figure 4b); for still smaller Δ, the initial positive and negative Gaussians overlap considerably, and this cancellation reduces the shoreline motion; in this case it is debatable whether the wave should be referred to as an N-wave at all.

We will first consider the extrema of shoreline position, and then the conditions under which these N-waves break down.

4.1.1. *Extrema of shoreline position*

Figures 5(a) and (b) illustrate how the 'shape' parameters of the N-wave, κ_2 and Δ, control the extremal values of $C_0(\lambda)$ and thus the maximum runup and drawdown of the shoreline. We recall from (2.15) and (4.9) that $\eta_{sh}(\lambda) = -C_0(\lambda) - S_1^2(\lambda)/8$, and that $C_0(\lambda) \sim 4ak^{1/4} Z_N(b)$. For our discussion, it is simplest to consider only the case $a > 0$ (a leading-elevation N-wave), noting that the linearity of shoreline extrema in a makes it easy to reinterpret the results for a leading-depression N-wave with $a < 0$. In this case, we have

$$\max_{\lambda} \eta_{sh} = \max_{\lambda}(-C_0) \sim -\min_{b}(-4ak^{1/4} Z_N(b)) = 4ak^{1/4} \max_{b} Z_N(b), \tag{4.10}$$

$$\min_{\lambda} \eta_{sh} = \min_{\lambda}(-C_0) \sim -\max_{b}(-4ak^{1/4} Z_N(b)) = 4ak^{1/4} \min_{b} Z_N(b). \tag{4.11}$$

Figure 5(a), then, describes the maximum runup height of the wave. For a positive Gaussian (i.e. $A_2 = 0$ and $a > 0$), this would be given, from (3.12), by $\max_\lambda \eta_{sh} = 1.5926ak^{1/4}$, corresponding to $\max_b Z_N(b) = 0.3982$. As the figure indicates (note the position of the contours at 0.39 and 0.398), for our 'landslide-generated' N-waves this value is only approached in the limit as Δ becomes large, so the following trough does not influence the leading peak which controls the initial (and dominant) runup. In general, the presence of the following trough always slightly reduces the runup, but this effect only becomes pronounced for $\Delta \lesssim 0.5$.

In contrast, the maximum drawdown of the shoreline (figure 5b) is generally substantially increased by the following trough compared to the value of $\min_\lambda \eta_{sh} = -0.7318ak^{1/4}$ (and thus $\min_b Z_N(b) = -0.183$) attained under the Gaussian wave: again note the position of the dashed contour in figure 5(b). Drawdown is enhanced most when the arrival of the trough coincides with the backwash which follows the initial runup, and so is at its greatest when Δ is a little less than 1; for this and greater

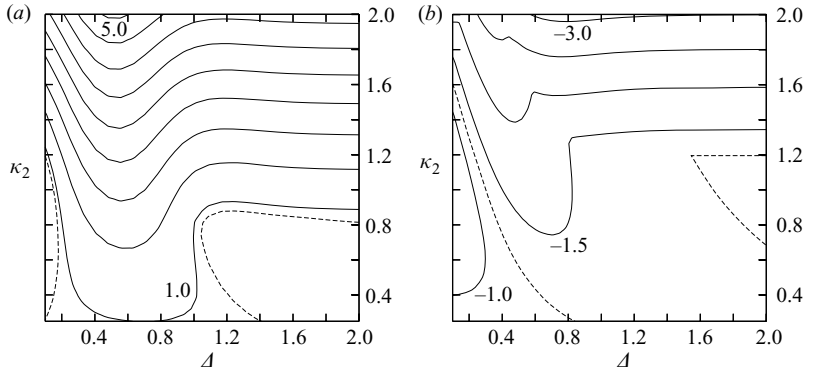

FIGURE 6. Breakdown conditions for the asymptotic solution for landslide-generated N-waves. (a) The maximum over b of $Z_N''(b) = I_2(b)/(16ak^{5/4})$: the dashed line is the contour at 0.891 (corresponding to the condition for the breakdown of a single positive Gaussian; solid lines are contours at 1 to 5 by 0.5. (b) The minimum over b of $Z_N''(b) = I_2(b)/(16ak^{5/4})$: the dashed line is the contour at -1.248 (corresponding to the condition for the breakdown of a single negative Gaussian); solid lines are contours at -1 to -3 by 0.5.

values of Δ, the following trough exerts a dominant control on drawdown, which consequently depends strongly on the trough steepness κ_2. (Conversely, a leading-depression N-wave may run up further than an estimate based on either the leading trough or the following peak would suggest.)

A final point which should be made, though, is that despite these cancellations and the overall complexity of the shoreline motion (figure 4), the variation of the values of the shoreline extrema as Δ and κ_2 are varied is not very great; except when Δ is very small and there is substantial cancellation, a very crude attempt to approximate the initial waveform by a single Gaussian corresponding to whichever of the two waves had the larger absolute amplitude would give estimates of the shoreline extrema which were correct to within a factor of order unity. This suggests that the details of the source are relatively unimportant if the overall amplitude and spatial extent of the initial waveform are known to reasonable accuracy.

4.1.2. *Conditions for solution breakdown*

Figures 6(a) and (b) illustrate how the shape parameters of the N-wave, κ_2 and Δ, control the extremal values of $C_2(\lambda)$ and thus the tendency of the wave solution to break down. Again we recall that the absolute amplitude and steepness of the wave enter only through the prefactor $ak^{5/4}$, and it is convenient to write the asymptotic estimate for C_2, using (4.9), as $C_2 \sim 16ak^{5/4}Z_N''(b)$. The condition for breakdown of a leading-elevation N-wave ($a > 0$) is then that $\max_b Z_N''(b) \geqslant 4/(16ak^{5/4})$, and for breakdown of a leading-depression N-wave ($a < 0$) that $\min_b Z_N''(b) \leqslant 4/(16ak^{5/4})$. Plotting contours of $\max_b Z_N''(b)$ and $\min_b Z_N''(b)$ in the (Δ, κ_2)-plane therefore describes how the shape parameters control the tendency of an N-wave to break down: the points on a given contour correspond to initial waveforms which will break down for a corresponding given value of $ak^{5/4}$. For comparison, we recall from (3.14) that a positive Gaussian wave ($a > 0$, $A_2 = 0$) breaks down if $14.26ak^{5/4} \geqslant 4$ and a negative Gaussian wave ($a < 0$, $A_2 = 0$) breaks down if $19.966ak^{5/4} \leqslant -4$: these correspond respectively to the contours marked in figure 6 with dashed lines, $\max_b Z_N''(b) = 0.891$ and $\min_b Z_N''(b) = -1.248$.

Bearing this in mind, we can interpret figure 6. The first point to remark is that only in small regions of parameter space (to the left of the leftmost branch, and below and to the right of the rightmost branch, of the dashed contour in each figure) is the value of $|a|k^{5/4}$ required for breakdown greater than that for the Gaussian wave. This confirms that the greater complexity of the N-wave, giving higher accelerations, makes N-waves more liable to break down than Gaussian waves. This applies for both leading-elevation and leading-depression waves (figures 6*a* and 6*b* respectively); another common feature of these plots is that in the regime $\Delta \gtrsim 1$, breakdown is dominated by the steeper and larger-amplitude wave, so the breakdown condition becomes almost independent of κ_2 for $\kappa_2 \lesssim 1$, and depends strongly on κ_2 for $\kappa_2 \gtrsim 1$. For lower values of Δ, the interaction between the two parts of the waveform becomes important. For a leading-elevation N-wave (figure 6*a*), breakdown is encouraged when the following trough coincides with the drawdown from the leading peak, reinforcing the high accelerations around maximum rundown; this tends to happen when Δ is around 0.5 to 0.6. For a leading-depression N-wave (figure 6*b*), there is a greater tendency for destructive interference between the leading depression and the following peak, which is particularly noticeable when κ_2 is small (a low and wide following peak). When the two waves are of similar dimensions, $\kappa_2 \approx 1$, breakdown is again encouraged by values of Δ around 0.5, but this tendency becomes less pronounced as the following wave comes to dominate at higher κ_2.

5. Discussion and conclusions

5.1. *Application to a tsunami event*

It is interesting to examine our results in dimensional form, using typical parameter values for tsunamis. There are obvious dangers in applying idealized mathematical models naïvely to complicated or ill-constrained field data, but such applications can be suggestive and provide useful physical insight. We will briefly consider two aspects of our results: the conditions for a tsunami to break down, with the likely formation of an incoming bore (q.v. Heller *et al.* 2005; Lavigne *et al.* 2007); and the ability of such a tsunami to mobilize rocky material on a beachface.

5.1.1. *Wave breakdown*

Taking the initial condition of a tsunami to be a positive Gaussian 'pulse' of the form considered in § 3, the condition for the shallow-water solution to break down is $a \gtrsim 0.28k^{-5/4}$. In dimensional terms, this becomes $\hat{a} \gtrsim (0.28 \tan\alpha)\hat{L}k^{-5/4}$, where the initial waveform is given by $\hat{\eta}(\hat{x}, 0) = \hat{a} \exp[-\hat{k}(\hat{x} - \hat{L})^2]$, $\hat{k} = k/\hat{L}^2$. Meanwhile, our asymptotic estimate of the maximum runup height $\hat{R}$ may be written, using (2.15) and (3.12), as $\hat{R} \sim 1.59\hat{a}k^{1/4}$.

We take as our prototype the earthquake-generated tsunami which struck the coast of Java on 17 July 2006. The source location for this tsunami is reasonably well constrained, and there were several surveys of runup heights in the immediate aftermath (e.g. Kongko *et al.* 2006; Cousins *et al.* 2006); it is notable that some eyewitness accounts suggest that this particular wave did break before reaching the beach, so the runup was controlled by a post-breaking bore (Lavigne *et al.* 2007). The offshore bathymetry is not, of course, precisely linear between the source and the shore: surveys (e.g. Kongko *et al.* 2006) indicate nearshore beach slopes of around 0.02–0.05, while the source was around 240 km offshore in water of the order of 3000 m depth; regional bathymetric charts suggest that the source–shore bathymetry is not monotonic, so we will consider only the propagation of the wave in the

monotonically shallowing region within 100 km or so of the shore. The horizontal scale of the initial disturbance appears to have been of the order of 10 km, while various models of the tsunami inception (DCRC 2006) suggest that the initial vertical displacement was of the order of 0.1–0.5 m.

In order-of-magnitude terms, then, we may take $\hat{L} \sim 10^5$ m, $\hat{k} \sim 10^{-8}$ m^{-2} (giving $k \sim 100$) and $\tan\alpha = 0.02$; the breakdown condition then becomes $\hat{a} \gtrsim 1.8$ m. This suggests that had the bathymetry been linear and laterally uniform, this particular wave should not have broken. However, the estimated maximum wave amplitude and that required for breakdown are rather similar in magnitude; there is clearly scope for breakdown to be induced and runup enhanced by local bathymetric focusing in the alongshore direction or by non-zero initial velocities (see § 3.4) or a more complicated initial waveform (see § 4.1), while it is also possible that eyewitness reports confused breaking of the tsunami with the breaking of long-period swell superimposed upon it. It is also suggestive that our asymptotic estimate of the runup height gives $\hat{R} \sim 0.5$–2.5 m for $\hat{a} \approx 0.1$–0.5 m, and these estimates are somewhat lower than the largest runup heights deduced from postevent surveys, which were up to 3.6 m in the survey by Kongko *et al.* (2006), 7 m in the survey by Pribadan *et al.* (2006), and 15.7 m in the survey by Lavigne *et al.* (2007). Again, this suggests that some focusing may have taken place, or even that the DCRC estimates of the initial displacement underestimated the tsunamigenic potential of the earthquake (as, for example, in the 'slow tsunami earthquakes' discussed by Polet & Kanamori 2000).

5.1.2. *Mobilisation of rocky material*

We may use the estimates for shoreline forces obtained in § 3.3 to comment on the ability of an incoming wave to transport material on the beachface, such as boulders. As a rough estimate, such a body will be moved if the drag and pressure-gradient forces acting on it are of the same order as its submerged weight $\hat{F}_w \sim \hat{D}^3(\hat{\rho}_p - \hat{\rho})\hat{g}$; this means that the maximum size of body which can be mobilized by drag forces is given by

$$\hat{D}_{max} \approx \frac{5.887 c_d \hat{\rho}}{(\hat{\rho}_p - \hat{\rho})} \frac{\hat{a}^2 k^{3/2}}{\hat{L}\tan\alpha}, \tag{5.1}$$

while pressure gradients can mobilize a body if

$$\frac{19.97\hat{\rho}}{(\hat{\rho}_p - \hat{\rho})} \frac{\hat{a}k^{5/4}}{\hat{L}} \gtrsim 1. \tag{5.2}$$

It is apparent from this that larger and smaller bodies may feel the effects of different forces and thus respond to different features of the hydrodynamics; this may partly explain why boulders and fine sediment appear to follow different transport patterns under tsunami currents, and why boulders do not follow the same sorting and grading trends as finer material (Dawson & Shi 2000).

If we consider rocky material, $\hat{\rho}_p \approx 2650$ kg m^{-3}, a typical form drag coefficient is $c_d = 1$. For the Javan event considered above, we have $k \sim 100$; and so we deduce that if $\hat{a} = 0.5$ m (giving runup distances of approximately the right magnitude), $\hat{D}_{max} \approx 0.45$ m. This is rather smaller than some boulders are reported to have been moved by other tsunamis (see, e.g., Nott 2003), and we note that the size of body which can be mobilized increases strongly with the amplitude of the wave. We have been unable to find reports of boulder mobilization by this tsunami, although it seems to have been capable of mobilizing material of a comparable size to our estimate, as Cousins *et al.* (2006) report that poorly-built brick buildings were largely destroyed

and the debris spread over the surrounding area. We also note that for this particular tsunami, the criterion (5.2) was not satisfied, meaning that pressure gradient forces are unlikely to have been important except near where wave breaking occurred.

5.2. *Summary and conclusions*

In this study we have derived relatively simple descriptions of the shoreline behaviour of long waves resulting from localized initial conditions: these supply estimates of runup distances and the forces exerted on bodies on the shore, and constrain the applicability of nonlinear shallow-water theory to this problem.

Starting from the general solution to the beach equations obtained by Carrier *et al.* (2003), we have shown how, by developing the near-shore expansion of Kânoğlu (2004), solutions for the hydrodynamic variables near the shoreline may be obtained by a single integration over a 'space-like' variable. Following Synolakis (1987), we have obtained asymptotic results for the shoreline hydrodynamics of the Gaussian waves introduced by Carrier *et al.* (2003), in the regime where the initial waves are localized. These results provide estimates for the maximum shoreline excursion and for the criterion for breakdown of the solution in this regime. Evaluating the full shoreline solution indicates in particular that the asymptotic estimates for breakdown are accurate for $k \gtrsim 2$, in other words for only moderately steep initial waveforms. Since the Gaussian profile is readily fitted to a wide range of initial conditions, these results may provide a rapid and effective means of estimating without detailed calculation whether the shallow-water solution for a given waveform will break down or not. Our scalings for Gaussian waves also provide new estimates of how the forces exerted by a tsunami depend on the size of the wave, which complement recent work using simpler hydrodynamic models (Luccio *et al.* 1998; Nott 2003). Finally, we have obtained equivalent results for N-waves comprising two Gaussians of opposite sign, quantifying the extent to which the more complicated initial waveform can increase the extrema of shoreline motion and accentuate the tendency of the wave to break down: breakdown is particularly likely when a trailing depression follows a wider leading peak, giving rapid accelerations around maximum drawdown.

There are clearly many aspects of tsunami hydrodynamics still to be explored; the results we have obtained on breakdown, as well as the observations reported by Lavigne *et al.* (2007), suggest that a particular priority should be to explore the fate of a wave once breakdown has occurred somewhere in the fluid domain, and the propagation of the ensuing bore. We suggest that this could be an important question to which further studies using the NSWEs could give part of an answer, by supplying the initial and boundary conditions for such a bore (see Guard, Baldock & Nielsen 2005). An additional area in which an asymptotic approach similar to ours could be informative is the runup of waves specified by boundary rather than initial data (Antuono & Brocchini 2007).

In conclusion, the results we have described illustrate a major strength of nonlinear shallow-water theory, which is its susceptibility to analysis, and they indicate the circumstances under which it is necessary to employ more detailed but expensive modelling approaches. We believe that they may provide a useful and relatively simple tool for researchers investigating the important problem of wave runup.

We are grateful to three anonymous referees for their many constructive comments and corrections, and for providing a preprint of the paper by Kânoğlu & Synolakis (2006); we are also indebted to the late Professor Howell Peregrine for his encouraging comments on an earlier version of this work. DP acknowledges the financial support

of NERC and EPSRC through a postdoctoral fellowship awarded under the EMS scheme (ref. NE/B50188X/1) and held at the BP Institute and Department of Earth Sciences, University of Cambridge. LD acknowledges the financial support of EPSRC through an MPhil studentship at the BP Institute and a PhD studentship at the University of Dundee.

REFERENCES

Antuono, M. & Brocchini, M. 2007 The boundary value problem for the nonlinear shallow water equations. *Stud. Appl. Maths* **119**, 73–93.

Carrier, G. F. & Greenspan, H. P. 1958 Water waves of finite amplitude on a sloping beach. *J. Fluid Mech.* **4**, 97–109.

Carrier, G. F., Wu, T. T. & Yeh, H. 2003 Tsunami runup and drawdown on a plane beach. *J. Fluid Mech.* **475**, 79–99.

Cousins, W. J., Power, W. L., Palmer, N. G., Reese, S., Tejakusuma, I. & Nugrahdi, S. 2006 South Java Tsunami of 17th July 2006: reconnaissance report. *Tech. Rep.* 2006/33. GNS Science.

Dawson, A. G. & Shi, S. 2000 Tsunami deposits. *Pure Appl. Geophys.* **157**, 875–897.

DCRC 2006 Modeling a tsunami generated by the July 17, 2006 earthquake south of Java, Indonesia. Disaster Control Research Centre, Tohoku university (published online at http://www.tsunami.civil.tohoku.ac.jp/hokusai2/disaster/06_Java/July17Java.html.)

Dickinson, L. 2005 The sedimentary signature of long waves on coasts. Master's thesis, University of Cambridge.

Dyer, K. R. 1986 *Coastal and Estuarine Sediment Dynamics*. Wiley.

Gradshteyn, I. S. & Ryzhik, I. M. 2000 *Table of Integrals, Series and Products*, 6th edn. Academic.

Greenspan, H. P. 1958 On the breaking of water waves of finite amplitude on a sloping beach. *J. Fluid Mech.* **4**, 330–334.

Grilli, S. T., Svendsen, I. A. & Subramanya, R. 1997 Breaking criterion and characteristics for solitary waves on slopes. *J. Waterway Port Coastal Ocean Engng* **123** (3), 102–112.

Guard, P. A., Baldock, T. & Nielsen, P. 2005 General solutions for the initial runup of a breaking tsunami front. In *Intl Symp. on Disaster Relief on Coasts*. Monash University, Australia.

Heller, V., Unger, J. & Hager, W. 2005 Tsunami runup – a hydraulic perspective. *J. Hydraul. Engng* **131** (9), 743–747.

Hoefel, F. & Elgar, S. 2003 Wave-induced sediment transport and sandbar migration. *Science* **299**, 1885–1887.

Jensen, A., Pedersen, G. K. & Wood, D. J. 2003 An experimental study of wave runup at a steep beach. *J. Fluid Mech.* **486**, 161–188.

Kânoğlu, U. 2004 Nonlinear evolution and runup–rundown of long waves over a sloping beach. *J. Fluid Mech.* **513**, 363–372.

Kânoğlu, U. & Synolakis, C. 2006 Initial value problem solution of nonlinear shallow water-wave equations. *Phys. Rev. Lett.* **97**, 148501.

Kongko, W. *et al.* 2006 Rapid survey on tsunami Jawa 17 July 2006. *Tech. Rep.* UNESCO Report (published online at http://ioc3.unesco.org/itic/files/tsunami-java170706_e.pdf.)

Lavigne, F., Gomez, C., Giffo, M., Wassmer, P., Hoebreck, C., Mardiatno, D., Prioyono, J. & Paris, R. 2007 Field observations of the 17 July 2006 tsunami in Java. *Nat. Haz. Earth Sys. Sci.* **7**, 177–183.

Luccio, P. A., Voropayev, S. I., Fernando, H. J. S., Boyer, D. L. & Houston, W. N. 1998 The motion of cobbles in the swash zone on an impermeable slope. *Coastal Engng* **33**, 41–60.

Meyer, R. E. 1986*a* On the shore singularity of water waves. I. The local model. *Phys. Fluids* **29**, 3152–3163.

Meyer, R. E. 1986*b* Regularity for a singular conservation law. *Adv. Appl. Math.* **7**, 465–501.

Nott, J. 2003 Waves, coastal boulder deposits and the importance of the pre-transport setting. *Earth Planet. Sci. Lett.* **210**, 269–276.

Peregrine, D. H. 1972 Equations for water waves and the approximations behind them. In *Waves on Beaches and Resulting Sediment Transport* (ed. R. E. Meyer), chap. 3, pp. 95–121. Academic.

Polet, J. & Kanamori, H. 2000 Shallow subduction zone earthquakes and their tsunamigenic potential. *Geophys. J. Intl* **142**, 684–702.

Pribadi, S., Fachrizal, I., Gunawan, I., Hermawan, I., Tsuji, Y. & Sub, S. 2006 Gempabumi dan tsunami selatan jawa barat, 17 juli 2006. *Tech. Rep.* BMG Jakarta, in Indonesian with English abstract. (Available online at http://aeic.bmg.go.id/file/Pangadaran_report_en.pdf.)

Synolakis, C. E. 1987 The runup of solitary waves. *J. Fluid Mech.* **185**, 523–545.

Tadepalli, S. & Synolakis, C. E. 1994 The runup of *N*-waves on sloping beaches. *Proc. R. Soc. Lond.* A **445**, 99–112.

Tinti, S. & Tonini, R. 2005 Analytical evolution of tsunamis induced by near-shore earthquakes on a constant-slope ocean. *J. Fluid Mech.* **535**, 33–64.

Titov, V. V. & Synolakis, C. E. 1998 Numerical modelling of tidal wave runup. *J. Waterway Port Coastal Ocean Engng* **124** (4), 157–171.

Yeh, H. 2006 Maximum fluid forces in the tsunami runup zone. *J. Waterway Port Coastal Ocean Engng* **132** (6), 496–500.